Ab initio-based exciton model of amide I vibrations in peptides: Definition, conformational dependence, and transferability

Roman D. Gorbunov, Daniil S. Kosov,[a] and Gerhard Stock[b]
Institute of Physical and Theoretical Chemistry, Johann Wolfgang Goethe University, Marie Curie Str. 11, D-60439 Frankfurt, Germany

(Received 24 January 2005; accepted 4 March 2005; published online 13 June 2005)

Various aspects of the *ab initio*-based parametrization of an exciton model of amide I vibrations in peptides are discussed. Adopting "glycine dipeptide" (Ac-Gly-$NHCH_3$) as a simple building-block model that describes the vibrational interaction between two peptide units, we perform comprehensive quantum-chemical calculations to investigate the effect and importance of the level of theory, the choice of local coordinates, and the localization method. A solvent continuum model description turns out important to obtain planar CONH peptide units when a full geometry optimization (which is necessary to obtain the correct frequencies) is performed. To study the conformational dependence of the amide I vibrations, we calculate (ϕ,ψ) maps of the local-mode frequencies and couplings. Performing conformational averages of the (ϕ,ψ) maps with respect to the most important peptide conformational states in solution (α, β, P_{II}, and C_5), we discuss the relation between these measurable quantities and the corresponding conformation of the peptide. Finally, the transferability of these maps to dipeptides with hydrophilic and hydrophobic side chains as well as to tripeptides with charged end groups is investigated. © *2005 American Institute of Physics*. [DOI: 10.1063/1.1898215]

I. INTRODUCTION

Secondary structures of peptides and proteins can be studied by infrared (IR) spectroscopy, using the structurally sensitive and strongly IR-active amide I (mainly C═O stretch) and amide II (mainly C–N and C–N–H bend) vibrational modes as conformational probes.[1,2] Employing empirical rules that relate frequencies of amide bands to secondary structures, structural motives such as α and 3_{10} helices as well as parallel and antiparallel β sheets have been identified. For example, Schweitzer-Stenner and co-workers have investigated the conformation of small peptides by using a combination of vibrational spectroscopies including Fourier transform IR, polarized Raman, and vibrational circular dichroism.[3–6] Recently, the advent of multidimensional IR techniques has revealed a wealth of novel and quite detailed information on the structure and dynamics of biomolecules.[7] Beautiful examples are the two-dimensional infrared studies of various small peptides by Hamm and Hochstrasser and their co-workers.[8–13] The interpretation of these experiments, however, is far more involved than for simple linear IR absorption and clearly requires substantial theoretical support.

A *first-principle* theoretical description of the IR response of a peptide in aqueous solution represents a considerable challenge. On one hand, the vibrational frequency splittings of interest are relatively small and their calculation requires accurate *ab initio* methods using large basis sets. On the other hand, the conformational dynamics of the peptide and the fluctuations of the solvent need to be taken into account, e.g., by a classical molecular-dynamics simulation of the complete system. Since a direct *ab initio* molecular-dynamics description of a solvated peptide is in general too expensive, various approximate strategies have been proposed. Assuming that the vibrational mode coupling among localized vibrations originates mostly from electrostatic interaction, various workers have employed the transition dipole coupling model[1,2] or multipole generalizations thereof.[14–16] However, these methods were found to fail in the case of next-neighbor coupling, where through-bond covalent interactions become important. Alternatively, it has been suggested to perform an *ab initio* description of small peptide "building block" models, which subsequently can be put together in order to describe larger systems.[14–24] The idea is similar to the exciton model, which has been widely employed to describe electronic excitations of extended systems composed of many similar repeat units, such as aggregates and molecular crystals.[25,26] It assumes that the vibrational normal modes of interest can be represented by vibrations of local peptide modes, which—in a first approximation—do not interact with the remaining vibrational degrees of freedom of the peptide. For example, to describe the amide I modes of a peptide, one could use the C═O stretch vibration of each peptide unit as local modes. The assumption of a separable amide I subspace reduces the full system, including all degrees of freedom, to an N-dimensional vibrational problem, where N is the number of amino acids. Recent *ab initio* calculations of the amide I anharmonic couplings indicate that this basic assumption of separability is surprisingly well fulfilled.[19,22,23,27] The vibrational exciton model therefore represents a practical computational approach, it provides a physically appealing picture of peptide vibrations in

[a]Current address: Department of Chemistry and Biochemistry, University of Maryland, College Park, MD 20742-4454.
[b]Electronic mail: stock@theochem.uni-frankfurt.de

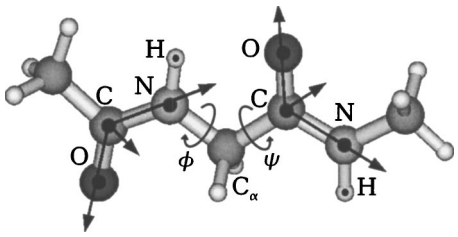

FIG. 1. Scheme of the "glycine dipeptide analog" (GD) molecule, introducing the two local coordinate systems, which are employed to define NMA-based amide I local modes of the system.

terms of local modes, and it can be employed to fit and interpret experimental IR spectra.[8,28–30]

As a simple building-block model that describes the vibrational interaction between two peptide units, several groups have considered the amide I vibrations of Ac-Gly-$NHCH_3$(CH_3–CONH–CH_2–CONH–CH_3), often referred to as glycine dipeptide (GD).[14,15,21,22,24] Employing various approaches, the off-diagonal vibrational coupling between the two peptide units as well as the diagonal force constants have been calculated as a function of the (ϕ,ψ) dihedral angles of the peptide backbone, see Fig. 1. For example, Torii and Tasumi[14] have reported an *ab initio*-based (ϕ,ψ) map of the amide I vibrational couplings, which was successfully employed to model two-dimensional infrared (2D-IR) experiments on trialanine.[10,12] To calculate these maps, several choices of local amide I modes have been suggested, including the C═O stretch vibrations and the normal modes of N-methylacetamide (CH_3–CONH–CH_3). Various ways to calculate the vibrational couplings and force constants for a given set of local modes have been proposed, including finite-difference differentiation[14] and the so-called Hessian matrix reconstruction method.[15,22] Furthermore, the effect of the solvent on the peptide amide I vibrations has been studied through *ab initio* calculations using a solvent continuum model[31,32] and by performing quantum electron structure calculations for various snap shots of the molecule and the surrounding water obtained from molecular-dynamics simulations.[33–38]

While the above-mentioned works on GD used different theory levels, basis sets, local coordinates, and localization schemes, it is not obvious to what extent the various approaches lead to a consistent and sufficiently accurate representation of the amide I vibrations. Furthermore, it is important to investigate the effect of the aqueous solvent on the (ϕ,ψ) map, i.e., to study if a geometry optimization for fixed (ϕ,ψ) with and without the solvent leads to comparable results. Finally, it has not yet been shown whether GD is really applicable as a building-block model. For example, it would be interesting to study the extent to which the (ϕ,ψ) maps are transferable to peptides with other side chains or other end groups. It is the goal of this paper to answer these questions.

To this end, we first perform test calculations using three levels of theory [Hartree–Fock, density-functional theory, and Møller–Plesset] and eight basis sets [from 6-31G(d) to 6-311++G(3df,2pd)]. Next, the choice of amide I local modes and its effect on the theoretical description is discussed in some detail. While both C═O stretch and NMA-based local modes provide a suitable representation of amide I vibrations, the latter choice requires that the CONH peptide units are constrained in a geometry optimization, which may lead to artifacts for some (ϕ,ψ) conformations of the peptide. C═O stretch local modes allow for a full optimization of geometry which, however, may lead to large nonplanarities of the CONH peptide units in the gas phase. Invoking a solvent continuum model is shown to resolve the problem, i.e., one can perform a full geometry optimization (which is necessary to obtain the correct frequencies), and at the same time obtain planar peptide unit geometries. To study the conformational dependence of the amide I vibrations, we calculate (ϕ,ψ) maps of the local-mode frequencies and couplings. Performing conformational averages of the (ϕ,ψ) maps with respect to the most important conformational states in solution (α, β, P_{II}, and C_5), we discuss the relation between these quantities measured in experiment and the conformation of the peptide. Finally, the transferability of these maps to dipeptides with hydrophilic and hydrophobic side chains as well as to tripeptides with charged end groups is investigated.

II. THEORY

A. Exciton model

It is useful to first summarize the main definitions associated with the vibrational exciton model (see Ref. 26 for a general introduction). For simplicity, we restrict the discussion to the special case of a peptide with two interacting amide I vibrations. Within the harmonic approximation, the Hamiltonian of two coupled oscillators can be written as

$$H = \frac{p_1^2}{2} + \frac{p_2^2}{2} + \tfrac{1}{2}k_1 q_1^2 + \tfrac{1}{2}k_2 q_2^2 + k_{12} q_1 q_2, \tag{1}$$

where q_1 and q_2 are mass-weighted local modes residing on the first and second peptide unit, respectively, and p_1 and p_2 are the corresponding conjugate momenta. The potential energy is characterized by the force constants k_1 and k_2 of the local modes as well as by the bilinear vibrational coupling k_{12}. In this work we are not concerned with the anharmonic potential terms of the exciton model, which have been introduced by several authors on an empirical[8] as well as on an *ab initio*[23] level, respectively.

To consider the normal modes $Q_{\mp}$ of the model, we introduce the unitary transformation

$$\begin{pmatrix} Q_- \\ Q_+ \end{pmatrix} = \begin{pmatrix} \cos\Theta & \sin\Theta \\ -\sin\Theta & \cos\Theta \end{pmatrix} \begin{pmatrix} q_1 \\ q_2 \end{pmatrix}, \tag{2}$$

with the mixing angle

$$\Theta = \tfrac{1}{2}\arctan\left[\frac{2k_{12}}{(k_1 - k_2)}\right], \tag{3}$$

which diagonalizes the Hamiltonian (1). This yields

$$H = \frac{P_-^2}{2} + \frac{P_+^2}{2} + \tfrac{1}{2}K_- Q_-^2 + \tfrac{1}{2}K_+ Q_+^2, \tag{4}$$

where Q_- and Q_+ are the two amide I normal modes with corresponding momenta P_- and P_+ and the force constants

$$K_\mp = \tfrac{1}{2}(k_1 + k_2) \mp \tfrac{1}{2}\sqrt{(k_1 - k_2)^2 + 4k_{12}^2}. \tag{5}$$

To make contact with the state representation commonly used in exciton theory, we introduce the harmonic-oscillator creation and annihilation operators

$$b_j^\dagger = (k_j^{1/4} q_j - i k_j^{-1/4} p_j)/\sqrt{2\hbar}, \tag{6}$$

$$b_j = (k_j^{1/4} q_j + i k_j^{-1/4} p_j)/\sqrt{2\hbar}, \tag{7}$$

where $j=1, 2$. The operators $b_j^\dagger$ and b_j create and destroy a localized vibration in the jth peptide unit with frequency $\sqrt{k_j}$, respectively, and satisfy the bosonic commutation relations $[b_i, b_j^\dagger] = \delta_{ij}$. Insertion into Eq. (1) yields

$$H = \varepsilon_1 b_1^\dagger b_1 + \varepsilon_2 b_2^\dagger b_2 + \beta(b_1^\dagger b_2 + b_2^\dagger b_1 + b_1^\dagger b_2^\dagger + b_2 b_1), \tag{8}$$

where

$$\varepsilon_i = \hbar\sqrt{k_i}, \tag{9}$$

$$\beta = \frac{\hbar k_{12}}{2(k_1 k_2)^{1/4}} \tag{10}$$

denote the energy of the ith site and the intersite coupling, respectively. Neglecting the nonresonant terms $b_1^\dagger b_2^\dagger$ and $b_2 b_1$, the Hamiltonian (8) reduces to the Frenkel exciton model[26]

$$H = (b_1\ b_2)\begin{pmatrix} \varepsilon_1 & \beta \\ \beta & \varepsilon_2 \end{pmatrix}\begin{pmatrix} b_1^\dagger \\ b_2^\dagger \end{pmatrix}, \tag{11}$$

which conserves the number of excitations. In this case, the system separates into blocks of the ground state, the one-exciton Hamiltonian, the two-exciton Hamiltonian, and higher terms (which are not of interest for the description of 2D-IR spectra). Diagonalizing the Hamiltonian (11), we obtain the normal mode frequencies

$$\Omega_\mp = \tfrac{1}{2}(\varepsilon_1 + \varepsilon_2) \mp \tfrac{1}{2}\sqrt{(\varepsilon_1 - \varepsilon_2)^2 + 4\beta^2}. \tag{12}$$

Note that the frequencies $\Omega_\mp$ obtained from Eq. (12) and $\omega_\mp = \hbar K_\mp$ obtained from Eq. (5) are not exactly the same,[39] which is a consequence of neglecting the nonresonant terms $b_1^\dagger b_2^\dagger$ and $b_2 b_1$ in Eq. (8). For amide I vibrations with $\beta/\varepsilon \ll 1$, these deviations are quite small, though, and can be safely neglected.

B. Local mode representation

While the above definition of the exciton model is a straightforward matter, it is not that clear how to consistently obtain the parameters of the model from quantum-chemical calculations. An *ab initio*-based parametrization of the exciton model Hamiltonian [Eq. (1)] for a specific system (say, GD) consists of two steps: (i) The identification of the local modes q_i and (ii) the calculation of the vibrational constants (e.g., k_i and k_{ij}). Since amide I vibrations consist mainly of C═O stretching, the C═O modes of the peptide backbone represent the simplest choice of amide I local modes. A more accurate description may be obtained by choosing the normal modes of N-methylacetamide (NMA) as local modes of a peptide unit.[14] A procedure to construct internal coordinates of GD that are easily expressed in terms of the NMA normal modes is introduced in Appendix A.

To explain the calculation of the vibrational constants, we first assume that we have performed a complete geometry optimization of GD. Choosing $(q_1, q_2) = (0,0)$ at the energy minimum, we perform a Taylor expansion of the total energy E with respect to q_1 and q_2, where the first derivatives $\partial E/\partial q_i$ vanish. The force constants k_1 and k_2 and the vibrational coupling k_{12} are then directly given by the second-order derivatives of the total energy, which can be computed via the finite-elements formula[40]

$$\begin{aligned} k_1 &= \frac{\partial^2 E(0,0)}{\partial q_1^2} = \frac{E(\Delta q,0) + E(-\Delta q,0) - 2E(0,0)}{\Delta q^2} \\ k_2 &= \frac{\partial^2 E(0,0)}{\partial q_2^2} = \frac{E(0,\Delta q) + E(0,-\Delta q) - 2E(0,0)}{\Delta q^2}, \\ k_{12} &= \frac{\partial^2 E(0,0)}{\partial q_1\, \partial q_2} = \frac{E(\Delta q_1, \Delta q_2) - E(-\Delta q_1, \Delta q_2)}{4\Delta q_1 \Delta q_2} \\ &\quad - \frac{E(\Delta q_1, -\Delta q_2) + E(-\Delta q_1, -\Delta q_2)}{4\Delta q_1 \Delta q_2}. \end{aligned} \tag{13}$$

Considering a general (i.e., nonequilibrium) conformation of GD characterized by the Ramachandran angles (ϕ, ψ), first a partial geometry optimization of GD with fixed (ϕ, ψ) is performed. Although the first derivatives are not exactly zero in this case, they are usually found to be small and presumably can be neglected. Hence, the vibrational constants are again given by the second-order derivatives in Eq. (13).

Alternatively, the vibrational constants can be calculated by invoking the amide I normal modes calculated for the full system. We denote these normal modes by X_- and X_+, in order to distinguish them from the normal modes $Q_\mp$ of the exciton model introduced in Eq. (2). Assuming that the amide I vibrations interact only weakly with the remaining vibrational modes of the peptide, the normal modes $X_\mp$ can approximately be related to the local modes $q_{1/2}$ by a unitary transformation, i.e.,

$$\begin{pmatrix} X_- \\ X_+ \end{pmatrix} \approx U\begin{pmatrix} q_1 \\ q_2 \end{pmatrix} = \begin{pmatrix} \cos\theta & \sin\theta \\ -\sin\theta & \cos\theta \end{pmatrix}\begin{pmatrix} q_1 \\ q_2 \end{pmatrix}. \tag{14}$$

Hence, provided the normal modes $X_\mp$ and the local modes $q_{1/2}$ are given, the transformation U can be constructed (see Appendix B), and the local-mode vibrational constants k_1, k_2, and k_{12} can be obtained from the normal-mode force constants $K_\mp$ through

$$\begin{pmatrix} k_1 & k_{12} \\ k_{12} & k_2 \end{pmatrix} = U^{-1}\begin{pmatrix} K_- & 0 \\ 0 & K_+ \end{pmatrix} U. \tag{15}$$

(Similarly, the site energies ε_1 and ε_2 as well as the coupling β of the Hamiltonian (11) are obtained from the normal-mode frequencies $\Omega_\mp$.) This approach, sometimes referred to

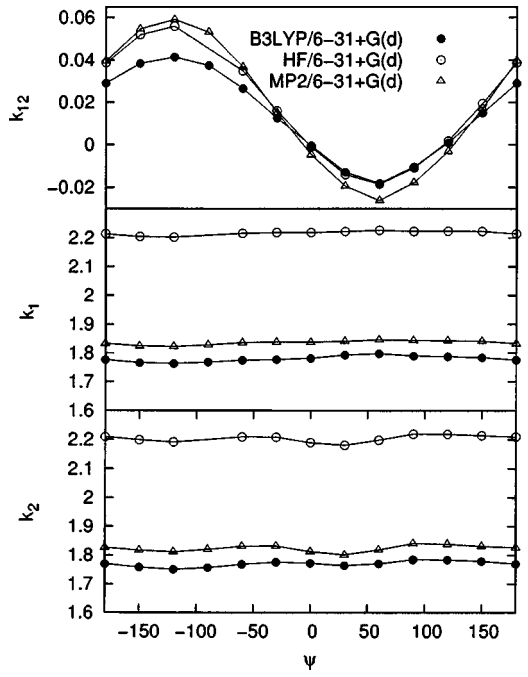

FIG. 2. Comparison of the amide I vibrational coupling k_{12} and force constant k_1 of GD as obtained for $\phi=-60°$ at three levels of theory: Hartree–Fock, density-functional theory, and Møller–Plesset perturbation theory.

as the "Hessian matrix reconstruction" method, has successfully been employed by several groups.[15,22,23] It is noted that a single normal-mode calculation appears less cumbersome than nine single-point calculations required in the finite-difference method. On the other hand, the finite-difference calculations only use the total energy of the system, which is a more direct quantity than the normal modes obtained from the diagonalization of the full Hessian matrix.

III. COMPUTATIONAL RESULTS AND DISCUSSION

A. Choice of level of theory and basis set

All calculations reported in this paper were performed using the GAUSSIAN suite of programs.[41] To study the importance of electron correlation for the calculation of amide I vibrations in peptides, we compare computations of GD obtained for three levels of theory: Hartree–Fock (HF), density-functional theory (DFT) with three-parameter Becke–Lee–Yang–Parr (B3LYP) functional,[42] and Møller–Plesset perturbation theory (MP2). In all cases, the 6-31+G(d) basis set is used. As a representative example, Fig. 2 shows the conformational dependence of the force constants k_1, k_2 and the vibrational coupling k_{12} as a function of the backbone dihedral angle ψ. The vibrational constants are calculated for NMA-based local coordinates, using the finite-differences method. Choosing $\phi=-60°$, the plots monitor the transition from an α_R-helical structure at $\psi=-60°$ to a poly(Gly)II (P_{II}) structure at $\psi=140°$.

The diagonal and off-diagonal vibrational constants are seen to depend in a different way on the theory level and on the peptide conformation, respectively. The vibrational coupling k_{12} is only a little affected by the level of theory chosen, but is a sensitive probe of the peptide conformation. The force constants k_1 and k_2, on the other hand, vary only weakly as a function of ψ. Depending on the level of theory, the curves are significantly shifted to each other, thus reflecting the degree of electron correlation taken into account by the method. Employing the recommended frequency scale factors (0.90 for HF, 0.99 for B3LYP, and 0.94 for MP2), however, all three levels of theory give similar results for the force constants.

To study the basis-set dependence of the amide I vibrations of GD, we chose DFT/B3LYP as level of theory. Table I compares the vibrational constants for selected conformations of GD (parallel and antiparallel β sheet as well as right- and left-handed α helices), as obtained for eight different basis sets from 6-31G(d) to 6-311++G(3df,2pd). Furthermore, the root-mean-square deviation (RMSD) of each basis set is given with respect to the 6-311++G(3df,2pd) data, using a total of 17 conformations (see caption). On the basis of RMSD results, two main observations can be made. First, it is noted that already with the smallest basis set 6-31G(d) the vibrational coupling k_{12} is given with a relative accuracy of $\approx$1%. The force constants k_1 and k_2, on the other hand, are found to be much more sensitive to the choice of the basis set. Second, while the addition of polarization functions does not significantly improve matters (compare, e.g., 6-31G(d) and 6-31G(d,p) results), even moderate basis sets supplemented by diffuse *s* and *p* orbitals to C, N, and O atoms yield results that are comparable with the 6-311++G(3df,2pd) reference calculations.

Due to these findings, DFT calculations using a 6-31G+(d) basis set and the B3LYP functional are chosen as a compromise between high accuracy and low computational effort. Based on the observation that the combination of the B3LYP functional with a 6-31+G(d) basis set leads to a maximally planar peptide group in NMA, this level of theory was also recently employed to compute amide vibrations of the alanine and glycine dipeptides.[24,43]

B. Comparison of localization methods

In order to define and parametrize the exciton model Hamiltonian (1), we have introduced above two approaches to calculate the vibrational constants (i.e., finite-difference and Hessian matrix reconstruction) and also considered two choices of local modes (i.e., C═O and NMA-based amide I modes). Moreover, we have discussed that the geometry optimization for a given peptide conformation (ϕ,ψ) can be performed with or without constraining the peptide units. The two cases will be referred to as partial and full geometry optimization, respectively.[44] Based on extensive B3LYP/6-31+G(d) calculations on GD, in the following we investigate the performance of these methods.

We begin by comparing the amide I normal modes as obtained from their direct calculation via the full Hessian matrix to the results obtained from the exciton model. Clearly, an appropriate model should reproduce the frequencies as well as the eigenvectors of the amide I modes. It is noted that the reconstruction of the Hessian matrix via Eq. (14) fulfills this requirement by construction, since we have assumed in Eq. (B1) that all angles of the transformation coincide (i.e., $\theta_{ij}=\theta$). To study the performance of the finite-

TABLE I. Basis-set dependence of the diagonal force constants k_1 and k_2 and the vibrational coupling k_{12} as obtained from DFT calculations on glycine dipeptide. Data are shown for the following conformations and Ramachandran angles (ϕ,ψ): Parallel β sheet β_P $(-119,113)$, antiparallel β sheet β_{AP} $(-139,135)$, right-handed α helix α_R $(-57,-47)$, and left-handed α helices α_{L1} (57,47) and α_{L2} $(90,-90)$. The root-mean-square deviation (RMSD) is computed with respect to the 6-311+G(2df,2p) data, using besides the five listed structures 12 additional conformations with $(\phi,\psi)=(-n\cdot 90,-m\cdot 90)$, with $n,m=1, 2, 3$. Units are mdyn/Å u.

Basis set		β_P	β_{AP}	α_R	α_{L1}	α_{L2}	RMSD
	k_{12}	0.006 76	0.010 79	0.017 92	0.017 93	−0.004 24	5×10^{-5}
6-31G(d)	k_1	1.866 7	1.869 7	1.855 1	1.855 0	1.866 7	0.2
	k_2	1.871 4	1.872 1	1.853 7	1.853 8	1.870 2	0.2
	k_{12}	0.006 36	0.010 36	0.017 91	0.017 90	−0.004 55	6×10^{-5}
6-31G(d,p)	k_1	1.861 5	1.864 5	1.850 0	1.850 2	1.861 7	0.1
	k_2	1.866 7	1.866 0	1.849 2	1.848 9	1.865 9	0.1
	k_{12}	0.006 37	0.010 73	0.019 99	0.019 99	−0.004 53	3×10^{-6}
6-31+G(d)	k_1	1.782 7	1.786 8	1.774 0	1.774 6	1.785 2	0.003
	k_2	1.790 1	1.791 8	1.770 7	1.770 3	1.788 4	0.003
	k_{12}	0.005 74	0.010 08	0.019 99	0.019 87	−0.004 61	6×10^{-6}
6-31+G(d,p)	k_1	1.779 5	1.781 4	1.770 1	1.770 5	1.780 7	0.002
	k_2	1.785 9	1.787 9	1.766 6	1.766 7	1.783 6	0.002
	k_{12}	0.006 19	0.010 36	0.020 88	0.020 69	−0.004 34	3×10^{-6}
6-311+G(d,p)	k_1	1.763 5	1.766 7	1.755 6	1.755 3	1.766 6	0.000 5
	k_2	1.770 8	1.772 3	1.752 7	1.752 0	1.769 4	0.000 6
	k_{12}	0.006 72	0.010 82	0.020 44	0.020 26	−0.003 52	8×10^{-7}
6-311+G(2d,p)	k_1	1.745 6	1.748 2	1.737 6	1.737 9	1.748 1	0.009
	k_2	1.754 2	1.755 3	1.735 2	1.734 1	1.751 9	0.009
	k_{12}	0.006 51	0.010 48	0.020 4	0.020 24	−0.003 70	1×10^{-7}
6-311+G(2df,2p)	k_1	1.757 9	1.761 8	1.751 1	1.750 4	1.761 1	0.002
	k_2	1.766 9	1.768 1	1.747 3	1.746 8	1.765 0	0.002
	k_{12}	0.006 54	0.010 51	0.020 37	0.020 28	−0.003 79	0.0
6-311++G(3df,2pd)	k_1	1.768 6	1.771 9	1.761 2	1.761 2	1.770 9	0.0
	k_2	1.777 4	1.7778	1.758 0	1.757 2	1.775 5	0.0

difference calculations, Fig. 3 compares the the normal-mode frequencies of the exciton model obtained by partial geometry optimization and finite-difference calculations to the results of direct normal-mode calculations. The amide I frequencies are plotted as a function of the dihedral angle ψ, choosing again $\phi=-60°$. Although both calculations clearly exhibit the same conformational dependence, we find a uniform redshift of $\approx 10\ \mathrm{cm}^{-1}$ of the finite-difference calculations. A closer analysis suggests that the latter effect is caused by the reduced mass assumed for the mass-weighted local modes q_1 and q_2 in Eq. (13). To obtain the correct frequencies, the reduced mass for the NMA normal modes needs to be slightly (1.8%) corrected, in order to account for the presence of the remaining atoms of GD. To consider the eigenvectors obtained from the two methods, Fig. 3 also compares the angle θ of the coordinate transformation (14) to the mixing angle Θ obtained from Eq. (B4). The angles are seen to be in excellent agreement, showing that the finite-difference calculations are able to accurately reproduce the eigenvectors.

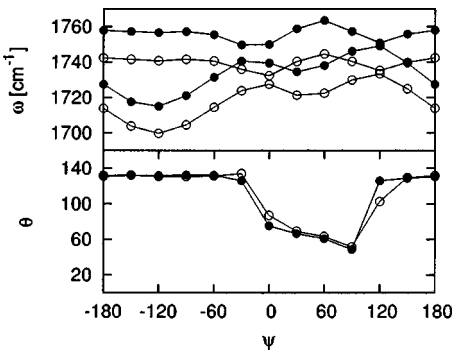

FIG. 3. Amide I normal-mode frequencies (upper panel) and mixing angle (lower panel) as functions of ψ computed along the line with fixed $\phi=-60°$. Compared are exciton-model results (empty circles) obtained by finite-difference calculations and the results from direct normal-mode calculations (full circles).

In conclusion, the Hessian matrix reconstruction method reproduces the correct normal-mode frequencies and eigenvectors by construction at the cost of a single normal-mode calculation. On the other hand, the finite-difference calculations reproduce the normal modes approximately and are somewhat more cumbersome since they require nine single-point calculations. It should be noted that finite-difference calculations represent a quite general approach to calculate vibrational coupling and only use the total energy of the system, which is a more direct quantity than the normal

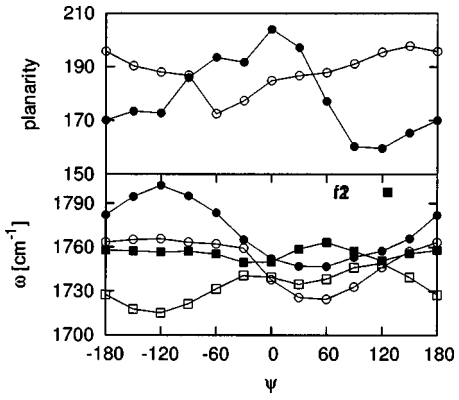

FIG. 4. Upper panel: Dihedral angles of the two CONH peptide units of GD obtained by full geometry optimization with fixed $\phi=-60°$, reflecting significant deviations from planarity (180°). Lower panel: Comparison of the amide I normal-mode frequencies of GD obtained for partial (squares) and full- (circles) geometry optimization.

modes obtained from the diagonalization of the full Hessian matrix. Nevertheless, for the applications considered here, the Hessian matrix reconstruction clearly appears to be advantageous.

Next we study the effect of the specific local modes chosen. To this end, we have compared vibrational constants calculated for C═O stretch and for NMA-based local modes, respectively, using partial geometry optimization and Hessian matrix reconstruction. Interestingly, it turns out that the two choices of local modes virtually yield the same results for the vibrational constants (data not shown). That is, our study of GD does not support the assumption that NMA-based local modes provide a better representation of amide I vibrations.

Finally, we wish to investigate the extent to which the vibrational properties depend on whether partial or full geometry optimization of the peptide has been performed.[44] Employing C═O local modes and Hessian matrix reconstruction, Fig. 4 shows the normal-mode frequencies obtained for the two cases, plotted as a function of the dihedral angle ψ, choosing again $\phi=-60°$. Interestingly, both absolute values and conformational dependence of the amide I frequencies are quite different in the two cases, revealing that constraining the CONH peptide units has a significant effect on the vibrational properties of the peptide. A closer analysis shows that the effect is mostly due to the fixed C–O bond length, which is known to be closely related with the amide I frequency.[22,23] Moreover, we have studied the structures of GD obtained by partial and full geometry optimization. As an example, Fig. 4 shows the dihedral angles of the two CONH peptide units (usually referred to as ω_1 and ω_2) obtained by full geometry optimization. The empty circles indicate the first peptide unit and filled circles the second one. Since 180° corresponds to planar peptide units, it is seen that the fully optimized calculations predict large nonplanarities for numerous peptide conformations (ϕ,ψ). On the other hand, by constraining the CONH peptide units during the optimization, the planarity is maintained by construction. To summarize, we find that the amide I frequencies as well as the geometry of the peptide depend sensitively on the kind of

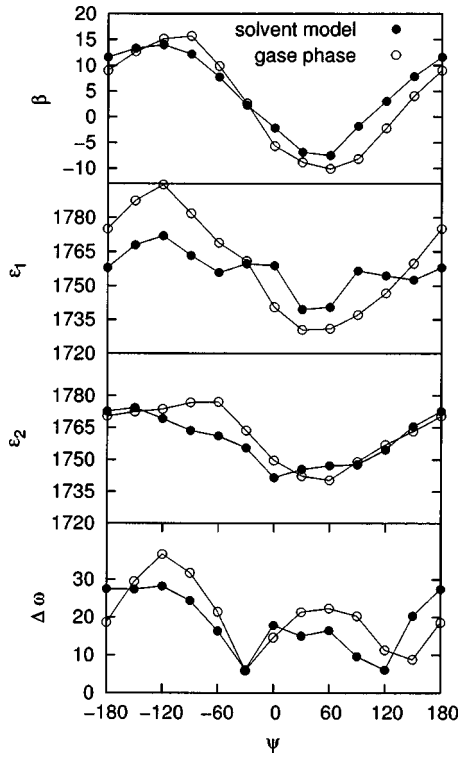

FIG. 5. Effect of a solvent continuum model on the amide I vibrational constants. Shown are (in cm^{-1}) the intersite coupling β, the site energies ε_1 and ε_2, as well as the frequency gap $\Delta\omega=\omega_+-\omega_-$, obtained for fixed $\phi=-60°$. For better comparison, the solvent-model values of the site energies have been up-shifted by 80 cm^{-1}.

geometry optimization. This somewhat disturbing observation suggests that it is necessary to improve upon the theoretical modeling.

C. Effect of the solvent

While the nonplanarity discussed above might be correct for the isolated peptide in gas phase, in aqueous solution one would certainly expect planar peptide groups. Hence, it is interesting to study whether the planarity of the fully optimized structures is regained when the effect of the solvent is approximately taken into account by a continuum model.[45] To this end, we have redone the fully optimized calculations employing the integral equation formalism polarized continuum model (IEF-PCM) solvent model[46] as implemented in GAUSSIAN03.[41] Interestingly, the solvent model calculations indeed showed that both CONH peptide units remained planar in the entire (ϕ,ψ) range, with dihedral angles ω_1 and ω_2 deviating at most a few degrees from 180° (data not shown).

Figure 5 reveals the effect of the solvent on the amide I vibrations by comparing gas-phase and continuum-model results of the intersite coupling β, the site energies ε_1 and ε_2, as well as the frequency gap $\Delta\omega=\omega_+-\omega_-$. As may be expected, the results for the intersite coupling and the frequency gap are only minorly changed by the solvent. In both cases, the overall conformational dependence is similar in the gas and the condensed phase, respectively, and the main effect of the solvent is to reduce the variation of the quantities (see also Fig. 9). The site energies, on the other hand,

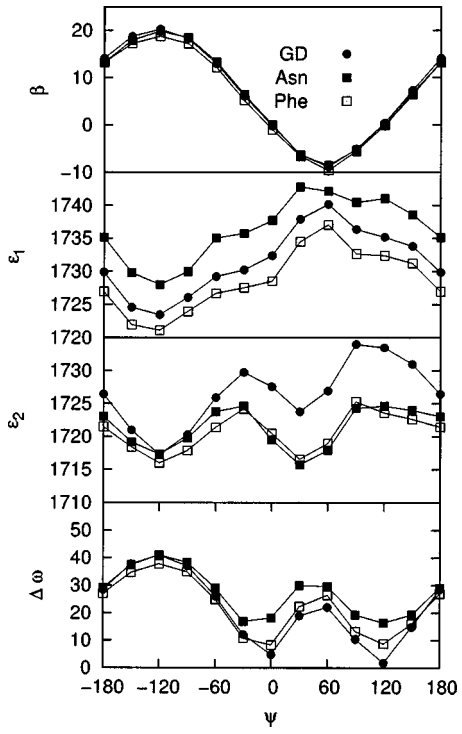

FIG. 6. Transferability of the amide I vibrational constants for Ac-Gly-$NHCH_3$ (GD) to peptides with a hydrophilic side chain Ac-Asp -$NHCH_3$ (Asp) and a hydrophobic side chain Ac-Phy-$NHCH_3$ (Phy), respectively. Shown are (in cm^{-1}) the intersite coupling β, the site energies ε_1 and ε_2, as well as the frequency gap $\Delta\omega=\omega_+-\omega_-$.

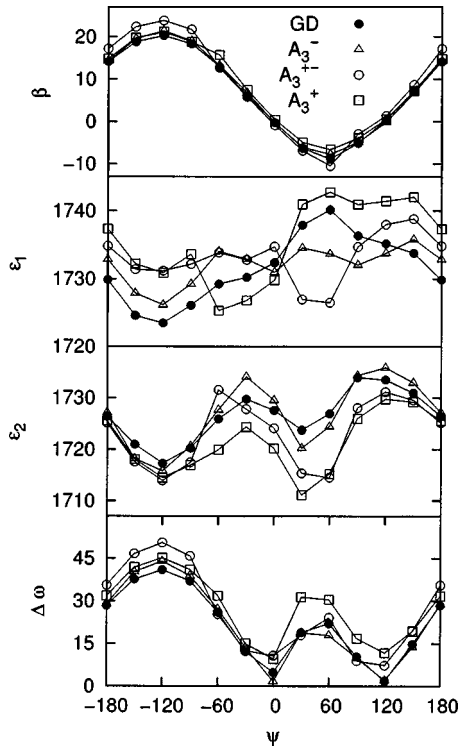

FIG. 7. Transferability of the amide I vibrational constants for Ac-Gly-$NHCH_3$ (GD) to trialanine in its zwitterionic (A_3^{+-}), cationic (A_3^+), and anionic (A_3^-) state. Shown are (in cm^{-1}) the intersite coupling β, the site energies ε_1 and ε_2, as well as the frequency gap $\Delta\omega=\omega_+-\omega_-$.

undergo an overall redshift of $\approx 80\ cm^{-1}$ upon solvation. Interestingly, the conformational dependence of the solution results for ε_1 and ε_2 is similar to the fully optimized gas-phase calculations, but clearly differs from the partially optimized results (cf. Fig. 4). This finding suggests that the former calculations are superior to the latter, although the fully optimized gas-phase results are plagued by nonplanar peptide geometries for some (ϕ,ψ) conformations.

D. Transferability of maps

It is interesting to investigate the extent to which the (ϕ,ψ) maps calculated above for GD (Ac-Gly-$NHCH_3$) are transferable to peptides with other side chains or end groups. With this end in mind, we have considered the systems Ac-Asp-$NHCH_3$ (as an example of a peptide with a hydrophilic side chain) and Ac-Phy-$NHCH_3$ (as an example of a peptide with a hydrophobic side chain). Plotted as a function of the dihedral angle ψ and $\phi=-60°$, Fig. 6 compares the vibrational constants obtained for the three dipeptide analogs. The intersite coupling β is almost identical in all three cases, showing again that this quantity is quite insensitive. Moreover, the frequency splittings $\Delta\omega$ are found to coincide nicely for all three dipeptide. The site energies ε_1 and ε_2, on the other hand, are somewhat shifted depending on the side chain, but nevertheless show quite similar conformational dependence.

To study the effect of various end groups, we have considered trialanine [which like GD is described by a single pair of flexible backbone dihedral angles (ϕ,ψ)] in its zwitterionic (A_3^{+-}), cationic (A_3^+), and anionic (A_3^-) state. As shown in Fig. 7, the intersite coupling β is hardly affected by the presence of the amino and carboxyl termini and by the different protonation states of trialanine. As may be expected, however, the site energies of trialanine only approximately match the results for GD. The frequency splitting $\Delta\omega$ again depends only weakly on the protonation state of trialanine. Assuming that trialanine occurs predominantly in the P_{II} conformation at $\psi=140°$,[10] we obtain $\Delta\omega\approx 20\ cm^{-1}$ for A_3^+ and A_3^{+-}, as well as $15\ cm^{-1}$ for A_3^-. This is in qualitative agreement with the experimental results $\Delta\omega\approx 25\ cm^{-1}$ for A_3^+ and A_3^{+-} and $11\ cm^{-1}$ for A_3^-.[3,4]

E. Conformational dependence of vibrational properties

Having established a suitable methodology, we are now in a position to discuss the conformational dependence of amide I vibrations of GD. To this end, Fig. 8 shows (ϕ,ψ) maps of the total energy E, the intersite coupling β, and the site energies ε_1 and ε_2. Employing Hessian matrix reconstruction and CO local modes, we compare the results obtained from partial (left) and full (middle) geometry optimization in the gas phase, as well as from a solvent-model calculation with full geometry optimization (right). Using a step size of 30° for the calculations, each map contains the raw data of 144 conformations, which subsequently were interpolated by employing a two-dimensional spline method.

Let us begin with the fully optimized gas-phase calculations of the total energy, which -in harmonic approximation-is given, including the zero-point energy correction and the entropic contribution for $T=300$ K. Similarly

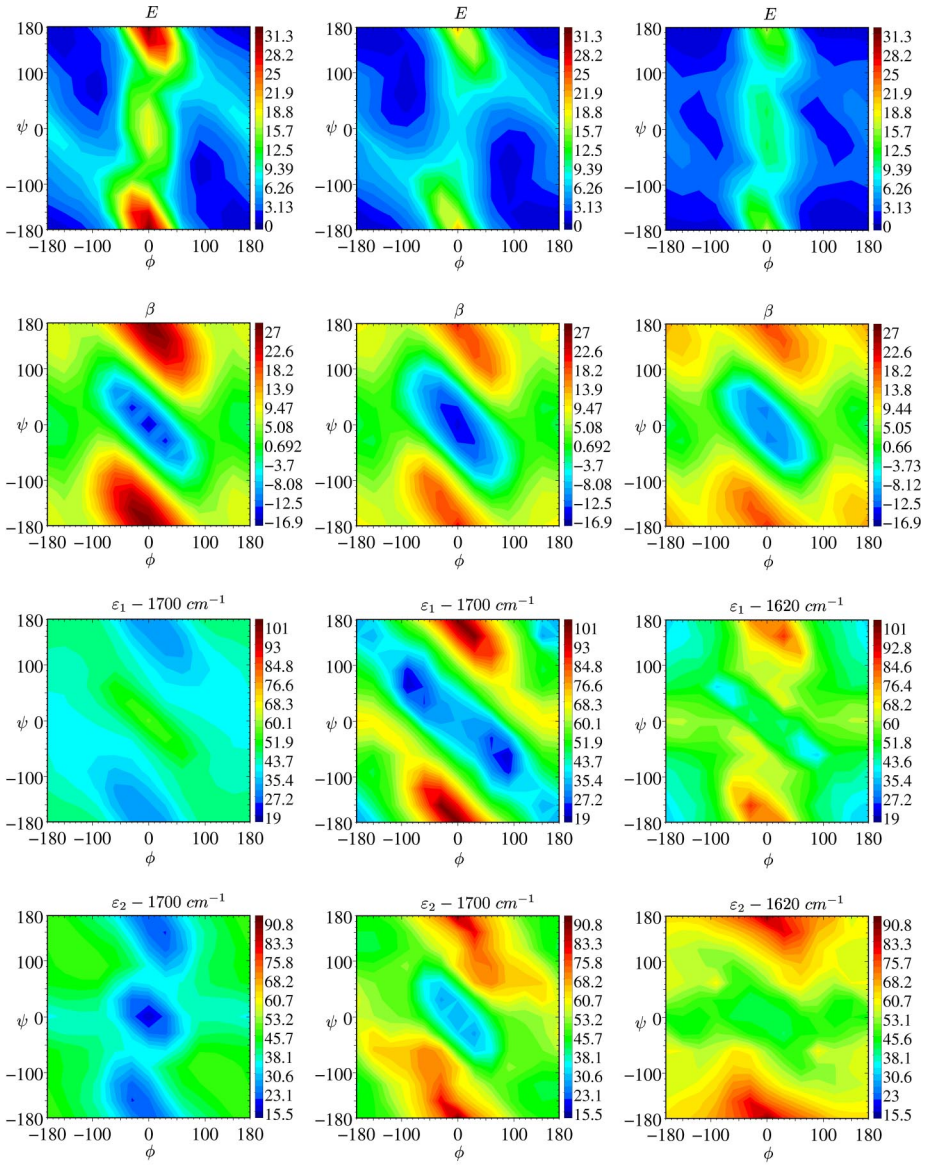

FIG. 8. (Color online). Conformational dependence of the total energy E (in kcal/mol) of GD, as well as of the amide I vibrational coupling β and the site energies ε_1 and ε_2 (in cm^{-1}). The maps are obtained from partial (left) and full (middle) geometry optimization in the gas phase, as well as from a fully optimized solvent-model calculation (right). For easier representation, the site energies were downshifted by 1700 cm^{-1} (gas phase) and 1620 cm^{-1} (solvent).

as observed by other authors,[21,24] we find three main minima; that is, at $(-90,60)$ and $(90,-60)$ we have two symmetry-related C_7 conformations, and at $(\pm 180°, \pm 180°)$ we have a planar fully extended C_5 conformation. As is expected from simple geometrical considerations of rigid GD,[47] the rotation along ϕ requires more energy than the rotation along ψ. While the ϕ rotation needs to overcome a steep barrier of ≈10–20 kcal/mol, the energy variations along ψ is significantly smaller (≈3–9 kcal/mol). Since GD has no massive side chain, only the conformations in the middle of the Ramachandran plot $(-50° < \phi < 50°)$ are significantly suppressed by the Boltzmann factor $\exp\{-E(\phi,\psi)/k_BT\}$. Comparing the fully optimized gas-phase calculations to results obtained by partial geometry optimization and by the fully optimized solvent continuum model, the total energy appears to be only minorly affected, but differs mainly in the height of the barriers. As is well-known,[31,32] continuum model approximations are not sufficient to stabilize the α-helical conformation which is found in explicit solvent.

Let us now consider the conformational dependence of the amide I vibrational coupling β. Since excitonic intersite couplings can—at least in principle—directly be measured in 2D-IR experiments,[10,48] their accurate calculation is a key to the structure determination of peptides via vibrational spectroscopy. As discussed by several authors,[14–16,21] the intersite coupling originates from both electrostatic (through space) and covalent (through bond) interactions. Although the overall (ϕ,ψ) dependence of β seen in Fig. 8 can be roughly explained by electrostatic modeling, the details as well as the correct values of the map require accurate *ab initio* calculations.

Roughly speaking, the vibrational coupling appears to depend only a little on the type of geometry optimization and on the inclusion of the solvent. Despite these similarities, the maps may yield different results when employed to calculate vibrational spectra. To point out these differences, it is instructive to evaluate the vibrational coupling for typical peptide structures as found in molecular-dynamics (MD) simu-

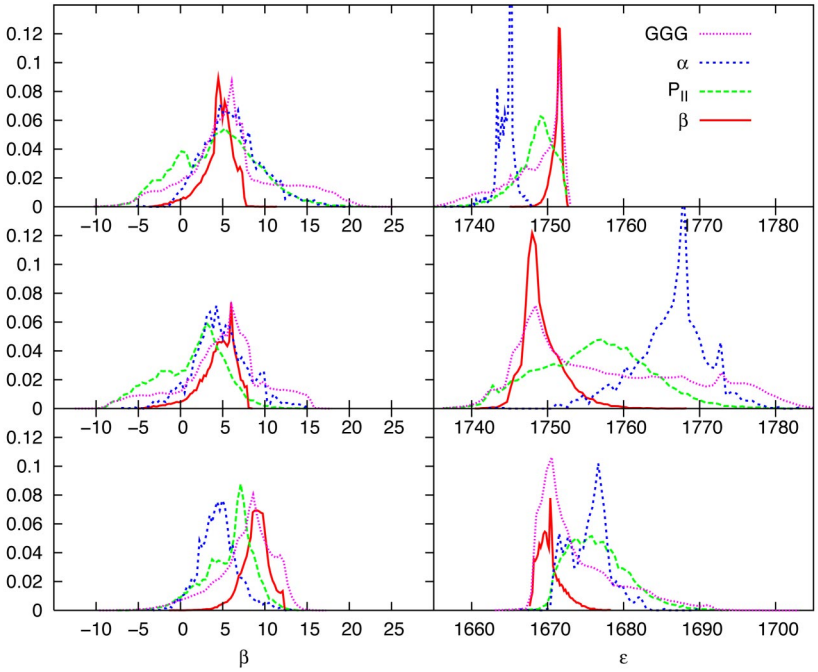

FIG. 9. (Color online). Probability distribution of the vibrational coupling β (left) and the average site energy $\varepsilon=\frac{1}{2}(\varepsilon_1+\varepsilon_2)$ (right), as obtained from conformational averages over the states α, β, P_{II}, and C_5, respectively. The results are obtained from partial (top) and full (middle) geometry optimization in the gas phase, as well as from a fully optimized solvent-model calculation (bottom).

lations. For the present study, the structures of the conformational states α, β, and P_{II} were taken from a MD study of trialanine in water,[49] the structures of the fully extended C_5 conformation were taken from a MD simulation of triglycine in water.[50] Using these data, Fig. 9 shows the probability distributions of β obtained from conformational averages over the states α, β, P_{II}, and C_5, respectively. The corresponding mean value $\langle\beta\rangle$ and the rms fluctuations $\delta\beta\equiv\langle(\beta-\langle\beta\rangle)^2\rangle^{1/2}$ of the coupling are listed in Table II. (Note that $\delta\beta^2$ is directly proportional to the vibrational energy transport rate along the peptide backbone, which was measured in 2D-IR experiments.[12]) Despite an overall similarity, the various distributions of β are certainly different and also lead to different averages. The main effect of the solvent model is a decrease of the conformational fluctuations of the coupling. Although there is a large overlap of the individual state-specific distributions, the vibrational coupling still reflects the conformation of the peptide.

We now turn to the discussion of the site energies ε_1 and ε_2, which are also shown in Fig. 8. As discussed by several authors,[21,23] the conformational dependence of these quantities cannot be easily explained by simple electrostatic considerations such as the transition dipole coupling model. Furthermore, we have seen throughout this paper that the site energies as well as the normal-mode frequencies are quite sensitive to all aspects of the theoretical description, including the level of theory, the basis set, and the method of localization. Considering the latter aspect, Fig. 8 shows that the maps obtained for partial and full geometry optimization differ considerably (for ε_1 even the maxima and minima are exchanged), while the solvent data agree at least roughly with the fully optimized gas-phase data.

This general picture is confirmed by Fig. 9, which displays the probability distributions of the average site energy $\varepsilon=\frac{1}{2}(\varepsilon_1+\varepsilon_2)$ as obtained from conformational averages over the states α, β, P_{II}, and C_5, respectively. An interesting ob-

TABLE II. Mean values and RMS fluctuations of various vibrational quantities as obtained from the averages over the conformational states α, β, P_{II}, and C_5. The data are generated from the corresponding (ϕ,ψ) maps for partial and full-geometry optimization, respectively. Units are in cm^{-1}.

Theory	State	β	ε_1	ε_2	ω_1	ω_2	$\Delta\omega$
Partially optimized	α	6.2±3.5	1743.4±2.0	1745.7±1.1	1737.4±4.0	1751.6±2.2	14.2±6.0
	β	4.5±1.8	1752.0±1.7	1750.3±0.8	1746.3±1.6	1756.1±1.5	9.8±2.8
	P_{II}	4.5±4.8	1747.4±3.3	1749.4±1.9	1742.5±6.0	1754.2±1.6	11.7±7.1
	C_5	6.2±5.5	1749.2±5.1	1748.5±3.3	1741.3±8.2	1757.6±3.3	14.5±9.0
Fully optimized	α	4.7±3.3	1767.2±5.0	1765.3±5.6	1759.4±3.8	1773.1±6.4	13.8±4.6
	β	4.5±2.2	1752.3±2.3	1746.4±4.6	1743.1±3.9	1755.5±2.2	12.4±3.2
	P_{II}	1.3±3.9	1759.3±4.2	1752.8±10.3	1749.6±8.3	1762.6±6.6	13.0±4.8
	C_5	4.9±4.9	1760.0±8.0	1756.3±14.2	1749.8±10.0	1766.6±12.3	15.9±6.3
Solvent	α	4.5±2.3	1677.7±3.7	1673.3±4.3	1668.2±2.1	1682.8±3.7	14.6±2.7
	β	8.8±1.6	1664.1±2.2	1676.5±2.9	1659.4±2.8	1681.2±2.7	21.8±4.4
	P_{II}	5.8±2.9	1673.7±4.6	1679.6±5.7	1669.0±3.0	1684.3±6.2	15.3±5.5
	C_5	7.7±3.4	1669.1±7.2	1678.4±5.4	1664.2±5.5	1683.9±6.7	19.6±6.3

servation can be made. Compared to the solvent data, the fully optimized gas-phase results are seen to reproduce the correct ordering of the peaks (e.g., the β and α conformations appear at the red and blue side of the energy spectrum), however, the width of the distributions are too large. On the other hand, the partially optimized gas-phase results give the correct width, but the wrong ordering. Hence the solvent model stabilizes the planarity of the CONH peptide units, which results in reduced conformational fluctuations similar to the partially optimized calculations. Moreover, the solvent model allows the C–O bond length to vary, which results in the correct amide I frequencies similar to the fully optimized calculations.

Finally, it is interesting to see the extent to which the solvent model results can be related to recent experimental data. Performing two-dimensional IR experiments on trialanine in aqueous solution, Woutersen *et al.* measured the vibrational energy transport rate along the peptide backbone.[10,12] Assuming constant site energies $\varepsilon_i(\phi,\psi)$ $=$const, they obtained the mean value $\langle\beta\rangle=6\ \mathrm{cm}^{-1}$ and the RMS fluctuation $\delta\beta=5.2\ \mathrm{cm}^{-1}$ of the vibrational coupling. As trialanine is mostly found in the P_{II} conformation,[13] the corresponding solvent-model results listed in Table II are $\langle\beta\rangle=5.7\ \mathrm{cm}^{-1}$ and $\delta\beta=2.8\ \mathrm{cm}^{-1}$. While the calculated mean vibrational coupling is in excellent agreement with experiment, its fluctuations appear to be underestimated. The latter is not necessarily a flaw of the present calculation, however, since the fluctuating site energies of the present model also affect the overall vibrational energy transport rate.[51] Furthermore, there has been some discussion on the reliability and accuracy of commonly used force fields applied to small and rather flexible peptides.[52–56] In the case of trialanine, for example, eight popular force-field parametrizations were compared,[52,56] which only in part were able to reproduce the experimental findings.[3,13,56]

Considering the linear IR absorption of triglycine and trialanine, amide I frequencies of $\approx$1660 and 1685 cm^{-1} for Gly_3^3 and $\approx$1650 and 1675 cm^{-1} for Ala_3^{10} have been obtained. The corresponding solvent-model results are 1664 and 1684 cm^{-1} for Gly_3 in the C_5 conformation and 1669 and 1684 cm^{-1} for Ala_3 in the P_{II} conformation. Taking into account that a continuum model represents a quite simple approximation of the solvent and that amide I frequencies depend in a subtle way on the various aspects of the theoretical description, the accuracy of the absolute frequencies appears satisfying. Interestingly, the calculations also somewhat underestimate the experimental frequency gap $\Delta\omega$ $\approx 25\ \mathrm{cm}^{-1}$, which represents a more robust quantity. This may be a consequence of the fact that the solvent-model calculations so far have been performed for neutral (but not zwitterionic) peptides. In experiments, on the other hand, ionic peptides are considered which, according to Fig. 6, exhibit larger frequency splittings.

IV. CONCLUSIONS

We have discussed various aspects of the *ab initio*-based parametrization of an exciton model of amide I vibrations in peptides. Adopting GD as a simple building-block model that describes the vibrational interaction between two peptide units, we have performed comprehensive DFT calculations to investigate the effect and importance of the level of theory, choice of local coordinates, and inclusion of the solvent. The main results of this study can be summarized as follows:

- DFT calculations using a 6-31G+(d) basis set and the B3LYP functional are a good compromise between high accuracy and low computational effort. This level of theory allows for a qualitatively correct characterization of the amide I vibrations in peptides.
- To calculate vibrational constants, the Hessian matrix reconstruction method appears to be advantageous over finite-difference calculations. This is because the former by construction reproduces the correct normal-mode frequencies and also requires less computational effort.
- Both types of local modes studied, C═O stretch and NMA-based modes, provide a suitable representation of amide I vibrations. C═O stretch modes are preferable, however, since NMA-based modes require that the CONH peptide units are constrained in a geometry optimization, which may lead to artifacts for some peptide conformations.
- Full optimization of geometry at fixed (ϕ,ψ) in the gas phase may lead to large nonplanarities of the CONH peptide units. On the other hand, the CONH peptide units remain planar in the entire (ϕ,ψ) range, if the effect of aqueous solvent is approximated by a continuum model.
- The main effects of a solvent continuum model on the amide I vibrations are an overall redshift of $\approx 80\ \mathrm{cm}^{-1}$ of the frequencies as well as an overall reduction of the conformational fluctuations of the vibrational constants. Furthermore, several details of the (ϕ,ψ) maps change upon solvation.
- Performing conformational averages of the (ϕ,ψ) maps with respect to the most important conformational states in solution (that is, α, β, P_{II}, and C_5), the site energies and the intersite coupling do reflect the conformation of the peptide, although there is a large overlap of the state-specific distributions.
- The (ϕ,ψ) maps of the vibrational coupling β as well as of the frequency splitting $\Delta\omega$ obtained for GD were found to be transferable to dipeptides with hydrophilic and hydrophobic side chains, as well as to tripeptides with charged end groups. The corresponding maps for the site energies match the results for GD only approximately.
- Generally speaking, the vibrational coupling is found to be quite robust with respect to most modifications under consideration. In contrast, the vibrational fre-

quencies depend sensitively on many details of the calculation.

The results listed above suggest various directions of further research. First, it remains to be investigated the extent to which the present building-block model is applicable to the study of the amide I vibrations of polypeptides. Furthermore, the fluctuations of the solvent may be included via an empirical model of the frequency shifts,[33–38] which can be evaluated along a molecular-dynamics trajectory. Doing so, it will be interesting to study if the highly averaged vibrational frequencies still depend that sensitively on the details of the calculation.

ACKNOWLEDGMENTS

The authors thank Peter Hamm, Yuguang Mu, Phuong Nguyen, and Hajime Torii for the inspiring and helpful discussions. This work has been supported by the Frankfurt Center for Scientific Computing, the Fonds der Chemischen Industrie, and the Deutsche Forschungsgemeinschaft.

APPENDIX A: CONSTRUCTION OF AMIDE I LOCAL MODES

We wish to construct internal coordinates of GD that can easily be expressed in terms of the normal modes of NMA. This projection procedure can be summarized as follows.

1. We begin with a full geometry optimization and a subsequent normal-mode analysis of the NMA molecule. Based on these calculations, the CONH peptide units and the methyl groups of GD are constrained to their NMA values. Moreover, the Ramachandran angles (ϕ,ψ) are fixed to represent the peptide conformation of interest.
2. The Z matrix of GD is constructed in terms of the two local coordinate systems shown in Fig. 1. For each CONH peptide unit, the origin of the coordinate system is located at the C atom, the first two axes are given by the C–O and C–N bonds, and the third axis is obtained by the cross product of the first two basis vectors. Since the CONH peptide units and the methyl groups are constrained, it is straightforward to express amide I vibrations of GD in terms of the local NMA coordinate systems.
3. Finally, a partial geometry optimization of GD with fixed (ϕ,ψ), CONH peptide units, and the methyl groups is performed, i.e., only the coordinates of two hydrogen atoms bonded to C_α and the lengths of the bonds N–C_α and C_α–C are optimized. The vibrational constants k_1, k_2, and k_{12} can then again be obtained from either finite-difference calculations or from the reconstruction of the Hessian matrix.

APPENDIX B: HESSIAN MATRIX RECONSTRUCTION

Let $\vec{n}_1$ and $\vec{n}_2$ be the amide I normal modes of the dipeptide, which are given as the 57-component vectors of atomic-mass-weighted Cartesian displacements in a GAUSSIAN output file for GD. We assume that these normal modes can be described by a linear combination of two local modes $\vec{l}_1$ and $\vec{l}_2$,

$$\begin{pmatrix}\vec{n}_1\\ \vec{n}_2\end{pmatrix}=\begin{pmatrix}\cos\theta_{11} & \sin\theta_{12}\\ -\sin\theta_{21} & \cos\theta_{22}\end{pmatrix}\begin{pmatrix}\vec{l}_1\\ \vec{l}_2\end{pmatrix}. \tag{B1}$$

The coefficients $\cos\theta_{ij}$ and $\sin\theta_{ij}$ are then given by the scalar products of normal and local modes, e.g.,

$$\cos\theta_{ij}=\frac{\vec{n}_i\cdot\vec{l}_j}{\vec{l}_j\cdot\vec{l}_j}. \tag{B2}$$

Assuming that the local modes are orthogonal to each other, we have $\theta_{11}=\theta_{12}$ and $\theta_{21}=\theta_{22}$, i.e., two angles can be eliminated. As it turns out, the remaining two angles are quite similar (e.g., $\theta_{11}\approx\theta_{22}$), and we can safely assume a single-transformation angle $\theta=(\theta_{11}+\theta_{22})/2$. Employing $\vec{n}_i$ and $\vec{l}_i$ as basis vectors to represent the normal modes $X_\mp$ and local modes $q_{1/2}$, respectively, Eq. (B1) reduces to the two-dimensional unitary transformation in Eq. (14). It should be noted that the definition of the local modes should not depend on the peptide conformation. To this end, for every conformation (ϕ,ψ) the Cartesian vectors $\vec{l}_i=\vec{l}_i(\phi,\psi)$ need to be rotated back to an arbitrary reference state $\vec{l}_i(\phi_0,\psi_0)$.

To compare amide I normal modes $X_\mp$ of the full system to the eigenvectors $Q_\mp$ of the exciton model, the angle θ of the coordinate transformation (14) is compared to the mixing angle Θ obtained from the vibrational constants via Eq. (3). In the latter equation Θ is defined in the range $[-45°,45°]$, while θ is considered in the range $[0°, 180°]$. To facilitate the comparison of the angles, we redefine Θ in the range $[0°, 180°]$ through the relation

$$k_{12}=\tfrac{1}{2}(K_+-K_-)\sin(2\Theta). \tag{B3}$$

According to Eq. (B3), the angle Θ is then defined as

$$\Theta=\begin{cases}\frac{1}{2}\arctan(2k_{12}/(k_1-k_2))+180° & \text{if } k_{12}>0 \text{ and } k_2-k_1>0\\ \frac{1}{2}\arctan(2k_{12}/(k_1-k_2))+90° & \text{if } k_{12}>0 \text{ and } k_2-k_1<0\\ \frac{1}{2}\arctan(2k_{12}/(k_1-k_2)) & \text{if } k_{12}<0 \text{ and } k_2-k_1>0\\ \frac{1}{2}\arctan(2k_{12}/(k_1-k_2))+90° & \text{if } k_{12}<0 \text{ and } k_2-k_1<0.\end{cases} \tag{B4}$$

[1] S. Krimm and J. Bandekar, Adv. Protein Chem. **38**, 181 (1986).
[2] H. Torii and M. Tatsumi, in *Infrared Spectroscopy of Biomolecules*, edited by H. H. Mantsch and D. Chapman (Wiley, New York, 1996), p. 1.
[3] R. Schweitzer-Stenner, F. Eker, Q. Huang, and K. Griebenow, J. Am. Chem. Soc. **123**, 9628 (2001).
[4] F. Eker, X. Cao, L. A. Nafie, and R. Schweitzer-Stenner, J. Am. Chem. Soc. **124**, 14 330 (2002).
[5] R. Schweitzer-Stenner, F. Eker, K. Griebenow, X. Cao, and L. A. Nafie, J. Am. Chem. Soc. **126**, 2768 (2004).
[6] F. Eker, K. Griebenow, X. Cao, L. A. Nafie, and R. Schweitzer-Stenner, Proc. Natl. Acad. Sci. U.S.A. **101**, 10 054 (2004).
[7] See Special Issue on *Multidimensional Spectroscopies*, edited by S. Mukamel and R. M. Hochstrasser [Chem. Phys. **266**, 135 (2001)].
[8] P. Hamm, M. Lim, and R. M. Hochstrasser, J. Phys. Chem. B **102**, 6123 (1998).
[9] M. T. Zanni, N.-H. Ge, Y. S. Kim, and R. M. Hochstrasser, Proc. Natl. Acad. Sci. U.S.A. **98**, 11 265 (2001).
[10] S. Woutersen and P. Hamm, J. Phys. Chem. B **104**, 11 316 (2000).
[11] S. Woutersen and P. Hamm, J. Chem. Phys. **114**, 2727 (2001).
[12] S. Woutersen, Y. Mu, G. Stock, and P. Hamm, Proc. Natl. Acad. Sci. U.S.A. **98**, 11 254 (2001).
[13] S. Woutersen, R. Pfister, P. Hamm, Y. Mu, D. S. Kosov, and G. Stock, J. Chem. Phys. **117**, 6833 (2002).
[14] H. Torii and M. Tasumi, J. Raman Spectrosc. **29**, 81 (1998).
[15] P. Hamm and S. Woutersen, Bull. Chem. Soc. Jpn. **75**, 985 (2002).
[16] A. M. Moran and S. Mukamel, Proc. Natl. Acad. Sci. U.S.A. **101**, 506 (2004).
[17] P. Bour and T. A. Keiderling, J. Am. Chem. Soc. **115**, 9602 (1993).
[18] P. Bour, J. Sopková, L. Bednárová, P. Malon, and T. A. Keiderling, J. Comput. Chem. **18**, 646 (1997).
[19] A. M. Moran, S.-M. Park, J. Dreyer, and S. Mukamel, J. Chem. Phys. **118**, 3651 (2003).
[20] J.-H. Choi, S. Ham, and M. Cho, J. Chem. Phys. **117**, 6821 (2002).
[21] S. Cha, S. Ham, and M. Cho, J. Chem. Phys. **117**, 740 (2002).
[22] S. Ham and M. Cho, J. Chem. Phys. **118**, 6915 (2003).
[23] H. Torii, J. Phys. Chem. A **108**, 7272 (2004).
[24] J. Antony, B. Schmidt, and C. Schütte, J. Chem. Phys. **122**, 014309 (2005).
[25] A. S. Davidov, *Theory of Molecular Excitons* (Plenum, New York, 1971).
[26] S. Mukamel, *Principles of Nonlinear Optical Spectroscopy* (Oxford University Press, Oxford, 1995).
[27] S. K. Gregurick, G. M. Chaban, and R. B. Gerber, J. Phys. Chem. A **106**, 8696 (2002).
[28] S. Woutersen and P. Hamm, J. Phys.: Condens. Matter **14**, 1025 (2002).
[29] R. Schweitzer-Stenner, J. Phys. Chem. B **108**, 16 965 (2004).
[30] S. Ham, S. Hahn, C. Lee, T.-K. Kim, K. Kwak, and M. Cho, J. Phys. Chem. B **108**, 9333 (2004).
[31] W.-G. Han, K. J. Jalkanen, M. Elstner, and S. Suhai, J. Phys. Chem. B **102**, 2587 (1998).
[32] K. J. Jalkanen, M. Elstner, and S. Suhai, J. Mol. Struct.: THEOCHEM **675**, 61 (2004).
[33] P. Bour and T. Keiderling, J. Chem. Phys. **119**, 11 253 (2003).
[34] S. Ham, J.-H. Kim, H. Lee, and M. Cho, J. Chem. Phys. **118**, 3491 (2003).
[35] K. Kwac and M. Cho, J. Chem. Phys. **119**, 2247 (2003).
[36] S. A. Corcelli, C. P. Lawrence, and J. L. Skinner, J. Chem. Phys. **120**, 8107 (2004).
[37] N. A. Besley, J. Phys. Chem. A **109**, 10 794 (2004).
[38] J. R. Schmidt, S. A. Corcelli, and J. L. Skinner, J. Chem. Phys. **121**, 8887 (2004).
[39] The units of force constants obtained from standard quantum-chemical programs are mdyn/(uÅ), while vibrational frequencies are usually given in cm^{-1}. The units are converted via $\omega[cm^{-1}]=1298.08\sqrt{K[mdyn/(uÅ)]}$.
[40] As a convention, we assume that local mode q_1 resides on the CH_3–NH–CO–C_α part of GD, while local mode q_2 resides on the C_α–NH–CO–CH_3 part.
[41] M. J. Frisch, G. W. Trucks, H. B. Schlegel, *et al.*, GAUSSIAN 03, Revision B.03, Gaussian, Inc., Pittsburgh, PA, 2003.
[42] A. D. Becke, J. Chem. Phys. **98**, 5648 (1993).
[43] N. G. Mirkin and S. Krimm, J. Phys. Chem. A **106**, 3391 (2002).
[44] To be precise, we note that the dihedral angles (ϕ,ψ) are fixed in the calculations referred to as "full geometry optimization."
[45] N. G. Mirkin and S. Krimm, J. Mol. Struct. **334**, 1 (1995).
[46] B. Mennucci and J. Tomasi, J. Chem. Phys. **106**, 5151 (1997).
[47] A. V. Finkelstein and O. B. Ptitsin, *Protein Physics. A Course of Lectures* (Academic Press, London, 2002).
[48] J. Bredenbeck, J. Helbing, R. Behrendt, C. Renner, L. Moroder, J. Wachtveitl, and P. Hamm, J. Phys. Chem. B **107**, 8654 (2003).
[49] Y. Mu and G. Stock, J. Phys. Chem. B **106**, 5294 (2002).
[50] J. Graf, P. H. Nguyen, G. Stock, and H. Schwalbe (upublished).
[51] R. D. Gorbunov, P. H. Nguyen, and G. Stock (unpubished).
[52] Y. Mu, D. S. Kosov, and G. Stock, J. Phys. Chem. B **107**, 5064 (2003).
[53] H. Hu, M. Elstner, and J. Hermans, Proteins **50**, 451 (2003).
[54] A. E. Garcia, Polymer **45**, 669 (2004).
[55] A. N. Drozdov, A. Grossfield, and R. V. Pappu, J. Am. Chem. Soc. **126**, 2574 (2004).
[56] S. Gnanakaran and A. E. Garcia, J. Phys. Chem. B **107**, 12 555 (2003).